ANALYSIS OF DEGRADED HYDROGEN DISSOCIATOR ENVELOPES BY AES*

Victor H. Ritz, Victor M. Bermudez, and Vincent J. Folen
Naval Research Laboratory
Washington, DC 20375

ABSTRACT

The performance of hydrogen dissociators used in atomic clocks is known to degrade after prolonged operation, requiring large increases in rf power to maintain a constant output of atomic hydrogen. Auger electron spectroscopy (AES) has been used to characterize the inner surfaces of Pyrex dissociator envelopes obtained from NASA Goddard Space Flight Center and Smithsonian Institution Astrophysical Observatory hydrogen masers. Prolonged operation of the dissociators leads to buildup of a dark film incorporating large quantities of carbon in its amorphous and carbide forms and smaller amounts of nitrogen. Possible mechanisms by which the film could interfere with the operation of the dissociator are given which involve its electrical conductivity and its role as a catalyst in the recombination of atomic hydrogen.

INTRODUCTION

A hydrogen maser will be used as a very accurate and stable frequency standard in a Navigation Technology Satellite (NTS-3) for the NAVSTAR Global Positioning System (GPS). The atomic hydrogen for the maser will be supplied by a dissociator of the type shown schematically in Fig. 1. The device operates by maintaining a rf glow discharge of ≈100 MHz in low pressure hydrogen gas admitted to the glass dissociator envelope. A gradual degradation in performance of such dissociators has been observed which apparently results from changes in the glass envelope after several months of operation. This degradation requires large increases in rf power to maintain a reasonable output of hydrogen atoms from the dissociator and limits its useful lifetime in satellite applications. The degradation is apparently connected with the concomitant darkening of the glass which is observed to occur as a light to dark brown film builds up on the inner surfaces of the dissociator. A photograph of a used dissociator envelope obtained from a Smith-

*Sponsored by The Naval Electronic Systems Command.

sonian Institution Astrophysical Observatory hydrogen maser is shown in Fig. 2. The arrow points to a dark brown discolored area. We have characterized such films by using Auger electron spectroscopy (AES) with in-depth sputter ion profiling. This paper will describe our recent measurements and summarize those obtained earlier [1].

EXPERIMENTAL TECHNIQUES AND RESULTS

Auger electron spectroscopy is a method of surface chemical analysis which is accomplished by energy analysis of the electrons ejected from a sample while it is bombarded with an electron beam [2]. The general arrangement of the apparatus (Physical Electronics Industries) is shown in Fig. 3. Samples are placed on a carrousel target holder and bombarded with monoenergetic electrons (3-5 kV) from either of the electron guns. The sample emits "Auger electrons" whose energies are characteristic of the atoms from which they were ejected. The Auger electrons are detected by the electron multiplier in the single pass cylindrical mirror analyzer and, after electronic processing, an Auger spectrum is displayed on an X-Y recorder. Since the Auger electrons which are detected come from the top few layers (i.e., depths of 10-20 Angstroms), AES is primarily a surface analytical technique. Information about the composition of the sample at greater depths can be obtained by ion-milling the surface with Argon ions from the sputter ion gun also shown in Fig. 3.

Our AES measurements were made with a Physical Electronics Industries cylindrical mirror analyzer (Model 10-155) operated at 5 kV in the derivative mode. The sample holder was oriented so the beam from the coaxial electron gun struck the dissociator glass at grazing incidence to minimize charging effects. The ultrahigh vacuum system was pumped down to $\approx 5 \times 10^{-10}$ Torr without bakeout before being backfilled with Ar for profiling with a PHI model 04-161 sputter-ion gun operated at 2 kV. An approximate calibration of the sputter-etch rate was obtained by profiling Ti films of known thickness deposited on glass substrates.

A typical AES spectrum for dissociator glass is shown in Fig. 4. The derivative of the number of electrons detected in each Auger peak by the analyzer is plotted as a function of the Auger electron energy. The various peaks have been labeled according to their corresponding elements. A quantitative chemical analysis may then be obtained from these raw peak heights by applying appropriate corrections. The elemental sensitivity factors of Palmberg et al. [3] obtained with the electron beam at 3 kV were scaled to 5 kV using correction factors measured in our apparatus for each element and SiO_2 . The raw Auger peak heights were processed with these sensitivity factors and summed over all the elements in the sample to obtain the atomic fraction of each element. The dissociator glass was Pyrex with a nominal composition (mol%) of 81% SiO_2, 13% B_2O_3, 4% Na_2O, and 2% Al_2O_3. Na was

rather difficult to detect reproducibly because of its high mobility during AES at room temperature [4], and a constant atomic fraction equal to 0.023 was assumed for it in summing the AES peaks.

In a dissociator of the NASA-Goddard configuration shown in Fig. 1, the rf power is introduced capacitively, and the glass surface immediately beneath the electrodes remains clear while the surrounding walls are darkened. Presumably, the sputtering action of the glow discharge near the electrodes continuously cleans the surface. Samples were cut from adjacent clear and slightly darkened areas of a degraded NASA-Goddard dissocator (sample 1) and subjected to AES analysis. The results are shown in Fig. 5. Both the atomic fraction and depth scales should be considered to be approximate. The upper half of the left side of Fig. 5 shows the main constituents of the clear portion of sample 1. O, Si, B, and Al are present in large concentrations which approach the nominal composition of Pryex (shown on the right-hand ordinate) after the contaminated surface layer has been sputter-etched away. A large amount of C is present on the surface which is removed fairly rapidly as the etching progresses. The lower half of Fig. 5 shows the elements present in smaller concentrations. The analysis of the slightly darkened portion of sample 1 is given on the right side of Fig. 5. It is distinguished by a very high C concentration on the surface which persists throughout the depth analyzed. N is also a prominent contaminant but at lower concentrations.

Samples of clear and darkened glass were also taken from another NASA-Goddard dissociator (sample 2). In this case, the darkened glass had a thick dark brown opaque film on it. AES was performed on the opaque film on the inner surface of the dissociator and also on the outer surface of an adjacent clear area as a check on the composition of a surface which had never been exposed to the glow discharge. Results for most elements parallel those for sample 1, and are shown in Fig. 6. Again, the primary difference was the presence of C and, to much lesser extent, N in the darkened glass.

In principle, the shape and position of the Auger peaks (e.g., Fig. 4) should yield some information about the chemical bonding in these films which are probably a mixture of amorphous C, SiO_2, SiC and Si_3N_4. The chemical bonding shifts which have been seen by other workers [5] [6] for the Si LVV and KLL peaks are shown schematically in Fig. 7. The Si_3N_4 LVV peak at 82 eV, is a shoulder of the main peak at 87eV, and moves to 80 eV when the Si_3N_4 is grown in the presence of oxygen [5]. Unfortunately, the close spacing of these shifts and the fact that several of these compounds were present simultaneously made it impossible for us to resolve them. Erratic charging of the sample to 5-10 Volts during analysis also contributed to the problem. More definitive results were obtained for C. Close inspection of the Auger spectra for the darkened portion of sample 1 revealed that the C peak changed from that characteristic of amorphous C[7] the "carbide type"

oberved by Grant and Haas [5]. Details of our Auger spectra for the amorphous and graphitic forms of C are shown in Fig. 8 along with the "carbide type" peak. We were thus able to distinguish between the amorphous and carbide forms of C as the films were sputter etched.

The atomic fractions of C in the clear and darkened portions of NASA-Goddard samples 1 and 2 are plotted in Fig. 9. The carbide peaks are designated by solid triangles. Figure 9 suggests that the surfaces of the dissociator fall into several categories. The clear outside surface of sample 2 incorporates very little C and no detectable N. This surface is easily cleaned of C by sputter etching and behaves in a way similar to that of a clean smooth microscope slide. The lightly darkened portion of sample 1 has a thin amorphous C layer on the surface and a persistent high concentration of carbide underneath it. A smaller concentration of N is also present. The clear portion of sample 1 under the electrodes has a layer of amorphous C and N which can be etched off fairly rapidly. The very thick opaque film analyzed in the darkened portion of sample 2 has amorphous C as its principal impurity along with smaller amounts of N. It does not etch off as easily, and has substantial amounts of C remaining at depths where the clear portions are quite clean.

AES was also performed on the dissociator from a Smithsonian Institution Astrophysical Observatory hydrogen maser which was operated continuously for 3 years at Maryland Point. This dissociator presented a variety of opaque discolorations which might be described as being milky, light brown, and dark brown. A milky portion of the inside of the dissociator was analyzed and compared to a portion of the outside. The most outstanding feature of the analysis was a heavy coating of amorphous C on the inside. The results are shown in Fig. 10 and generally parallel those of Fig. 9. Note that the film has been sputter-etched to a much greater depth and appears to be 1000-2000 Angstroms thick.

In addition to AES, some optical studies were made of the dissociator films. Optical spectra were obtained in the so-called "window" region of the glass substrate in the wavelength range between 300 nm and 4μ. Optical studies of NASA-Goddard dissociator sample 1 in the visible are shown in Fig. 11. The darkened glass in characterized by a structureless absorption edge monotonically rising from a low value in the near infrared to a high value in the ultraviolet. The results in the visible are similar to the broad background observed by Mattern et al. [8] in the course of H^+ - implantation experiments on fused silica and attributed to beam-assisted formation of a carbon film from organic contaminants. The assignment of the darkening to a carbon deposit is also supported by the proton irradiation work of Greer and Hapke [9], who point out that this absorption may be partly due to radiation-induced color center formation in the glass. However, the dominant effect would seem to be C-film buildup.

Optical measurements in the infrared are shown in Fig. 12 for portions of NASA-Goddard dissociator sample 1. The difference in transmission between the clear (1) and dark brown (2) samples indicates the presence of a weak band at $\approx 3240\ cm^{-1}$; i.e. 3.1μ. This band disappeared when the dark brown sample was scraped to remove the film (3) and was therefore intrinsic to the film. The band is too low in energy to be assigned to the O-H stretching vibration in isolated Si-OH or C-OH groups ($3600 - 3750cm^{-1}$) [10] and is lower in energy than the band observed in H^+ -implanted fused silica ($3680cm^{-1}$) [6]. It is, however, higher in energy than the C-H stretching vibration in alkanes or alkenes ($2800 - 3100cm^{-1}$) and the Si-H mode in silanes ($2150 - 2250cm^{-1}$) [10]. The band falls within the range expected for hydrogen-bonded O-H groups but is too sharp in comparison with the broad, asymmetric band which results from internal O-H groups in the glass ($3600cm^{-1}$). Si_3N_4 films formed by decomposition of gaseous mixtures of SiH_4 and NH_3 show a band at about $3340cm^{-1}$, assigned to the impurity N-H stretching vibration [11]. Since the dissociator film contains a high concentration of N, this is a possible explanation for the infrared data. Furthermore, the $3240cm^{-1}$ band lies within the range of C-H stretching frequencies in alkynes (monosubstituted acetylenes, $3200 - 3350cm^{-1}$) [10], in which the bonding orbitals on the carbon are in s-p hybridization. If this latter interpretation is correct, it indicates the presence of highly unsaturated carbon - carbon bonds in the film, which may be an important contribution to its photoconductivity.

DISCUSSION

Our experimental results indicate that the darkening of the glass dissociator envelope is caused by the formation of a composite film incorporating large quantities of C in its amorphous and carbide forms and smaller amounts of N. There are two general mechanisms by which formation of the film can interfere with the operation of the hydrogen dissociator: The electrical conductivity of the film can be high enough to exclude a fraction of the rf field, or the film can catalyze the recombination of hydrogen atoms.

The room temperature dc conductivity of various appropriate materials is given in Table I. It is seen that the dc conductivity of graphite ($\approx 7x10^{2}\ ohm^{-1}-cm^{-1}$) is much less than that of Cu ($\sim 6x10^{5}$). Measurements on amorphous C films [12] have shown even lower conductivity ($\approx 10\ ohm^{-1}-cm^{-1}$), as have Si_3N_4 ($2x10^{-6}\ ohm^{-1}cm^{-1}$) and amorphous SiC ($10^{-2}$ to $10^{-4}\ ohm^{-1}-cm^{-1}$). However, higher values ($\approx 3x10^{-3}$) have been observed for SiC doped with ≈ 0.005 atomic fraction of N [13]. Using the latter value, one may calculate the classical skin depth to be $\approx 100\ \mu$ at 100 MHz, and a rather thick film would be required to attenuate the rf input to the dissociator. One might also note that a large impurity photoconductivity has been observed in SiC [14], although no similiar data are available for impure carbon. Thus it is

possible that the conductivity of the composite film on the dissociator walls is higher than indicated in Table I under actual operating conditions when illuminated by the hydrogen glow discharge. In general, however, it would appear that very thick films would be required to effectively exclude the rf field.

Either direct or catalyzed reaction of the atomic hydrogen at the film would result in decreased output from the dissociator as the film is deposited. The principal reaction product of direct reaction of atomic hydrogen with carbon is known to be CH_4 and its rate of reaction with molecular H_2 is negligibly small below 1000°C [15]. However, King and Wise [16] have found that the direct reaction is a minor process in the carbon-atomic hydrogen system below 200°C and accounts for no more than 0.5% of the hydrogen atom removal. At higher temperature, the direct reaction increases but is still much smaller than catalytic recombination of the hydrogen atoms at the carbon film. It should be pointed out that the low pressures under which the dissociators operate ensure that recombination at the walls is much larger than in the volume of the gas itself.

There is a great variation in literature values of the heterogeneous recombination coefficient γ, defined as the fraction of atoms striking the surface that recombine. The discrepancies among values for the same material result from differences in thermal and chemical history and in surface roughness and contamination. A summary of values which have been obtained by various workers is given in Table II. Values for γ at room temperature of $\approx 580 \times 10^{-5}$ for Pyrex and of $\approx 1000 \times 10^{-5}$ for an evaporated C film have been obtained by Wise and coworkers [16][17]. More recently, values of $\approx (5\text{-}50) \times 10^{-5}$ have been measured for clean Pyrex and fused silica, while studies of pyrographite and electrode graphite have yielded values from 5000-10,000 $\times 10^{-5}$ [18]. Thus, a contaminating C film can be expected to increase the efficiency of recombination via atom-wall collision by at least a factor of 2 and perhaps by as much as a factor of 10-100.

Some possible sources of the C which builds up on the hydrogen dissociator walls are the residue left by inadequate initial cleaning of the glass, pump oil, CO, CO_2 or CH_4 outgassed from the walls and O-rings and the breakdown of epoxy cement into its constituents. Steps to minimize the influence of these sources would seem to be a sensible precaution in any hydrogen dissociator to be used for long periods of time.

ACKNOWLEDGEMENTS

The authors thank H. Peters and R. Vessot for providing samples of used dissociator chambers from NASA-Goddard Space Flight Center and Smithsonian Institution Astrophysical Observatory hydrogen masers, respectively. D.L. Griscom provided the drawing used as Figure 1.

REFERENCES

[1] V.H. Ritz, V.M. Bermudez, and V.J. Folen, J. Appl. Phys., 48, 2096 (1977).

[2] For a review see C.C. Chang, in Characterization of Solid Surfaces, (Plenum Press, New York, 1974), Ed. by P. Kane and G. Larrabee, pps. 509-561.

[3] P.W. Palmberg, G.E. Riach, R.E. Weber, and N.C. MacDonald, Handbook of Auger Electron Spectroscopy (Physical Electronics Industries, Edina, Minn., 1972).

[4] C.G. Pantano, D.B. Dove, and G.Y. Onoda, J. Non-Cryst. Solids 19, 41 (1975).

[5] P.H. Holloway, Surface Sci. 54, 506 (1976).

[6] J.T. Grant and T.W. Haas, Phys. Lett. 33A, 386 (1970).

[7] R. Ducros, G. Piquard, B. Weber, and A. Cassuto, Surface Sci. 54, 513 (1976).

[8] P.L. Mattern, G.J. Thomas, and W. Bauer, J. Vac. Sci. Technol. 13, 430 (1975).

[9] R.T. Greer and B.W. Hapke, J. Geophys. Res. 72, 3131 (1967).

[10] L.J. Bellamy, "Advances in Infrared Group Frequencies" (Methuen, London, 1968).

[11] Yu. I. Prokhorov, V.A. Sologub and B.A. Sukhodaev, Zh. Prikl. Spektr. 19, 520 (1973) - Engl. Transl.: J. Appl. Spectr. 19, 1211 (1973).

[12] M. Morgan, Thin Solid Films 7, 313 (1971).

[13] G.A. Slack and R.T. Scace, J. Chem. Phys. 42, 805 (1965).

[14] G. Jungk, K. Thiessen, and F. Witt, Phys. Status Solidi 3, 735 (1963).

[15] R.K. Gould, J. Chem. Phys. 63, 1825 (1975); B. McCarroll and D.W. McKee, Carbon 9, 301 (1971); Y. Sanada and N. Berkowitz, Fuel 48, 375 (1969).

[16] A.B. King and H. Wise, J. Phys. Chem. 67, 1163 (1963).

[17] B.J. Wood and H. Wise, J. Phys. Chem. 66, 1049 (1962).

[18] V.A. Lavrenko et al, Sov. Powder Metall. and Metal Ceram. 4(64), 320 (1968).

TABLE I

D.C. CONDUCTIVITY OF
VARIOUS MATERIALS

Material	σ in ohm^{-1} cm^{-1}
Copper[a]	6×10^5
Graphite[a]	7×10^2
Amorphous Carbon Film[b]	10
Silicon Nitride[c]	2×10^{-6}
Amorphous SiC Film[d]	10^{-2} to 10^{-4}
SiC with 0.5% Nitrogen[e]	3×10^3

a. "Handbook of Chemistry and Physics — 54th Ed." (C. R. C. Press, Cleveland, 1973), p. F-155

b. M. Morgan, Thin Solid Films 7, 313 (1971)

c. A. V. Gritsenko et al., Microelectronics 5, 170 (1976)

d. G. V. Bunton, J. Phys. D 3, 232 (1970)

e. G. A. Slack and R. I. Scace, J. Chem. Phys. 42, 805 (1965)

TABLE II

RECOMBINATION COEFFICIENTS FOR ATOMIC HYDROGEN

Material	γ
Vycor[a]	7×10^{-5}
Pyrex[b]	60×10^{-5}
Pyrex[c]	70×10^{-5}
Pyrex[d]	580×10^{-5}
Carbon Film[e]	$1{,}000 \times 10^{-5}$
Pyrographite[f]	$\approx 6{,}800 \times 10^{-5}$
Electrode Graphite[f]	$10{,}000 \times 10^{-5}$
Silicon Carbide[g]	$2{,}400 \times 10^{-5}$

a. A. Mandl and A. Salop, J. Appl. Phys. 44, 4776 (1973)

b. M. Coulon et al., J. Chim. Phys. 70, 1193 (1973)

c. G. A. Melin and R. J. Madix, Trans. Faraday Soc. 67, 2711 (1971)

d. B. J. Wood and H. Wise, J. Phys. Chem. 66, 1049 (1962)

e. A. B. King and H. Wise, J. Phys. Chem. 67, 1163 (1963)

f. V. A. Lavrenko et al., Sov. Powder Metall. and Metal Ceram. 4(64), 320 (1968)

g. V. A. Lavrenko et al., Dopov. Akad. Nauk Ukr. RSR, Ser. B, 30(3), 262 (1968)

LIST OF FIGURES

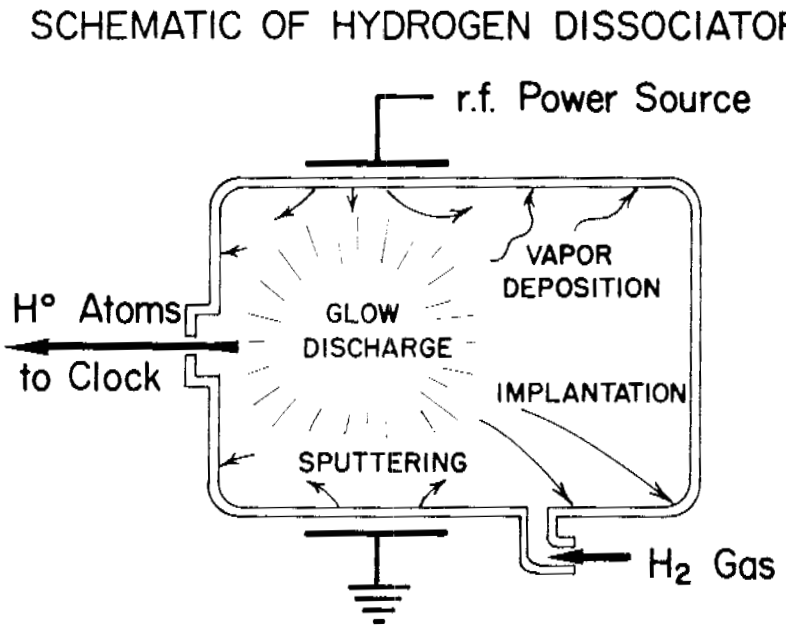

Fig. 1 Dissociator for production of atomic hydrogen.

Fig. 2 Discolored portion of S.A.O. dissociator.

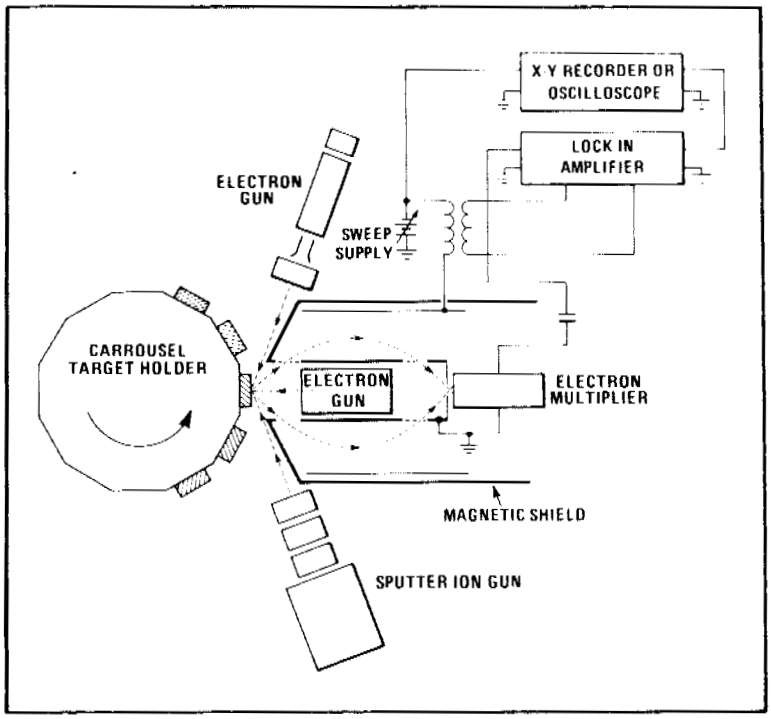

Fig. 3 Apparatus for Auger Electron Spectroscopy.

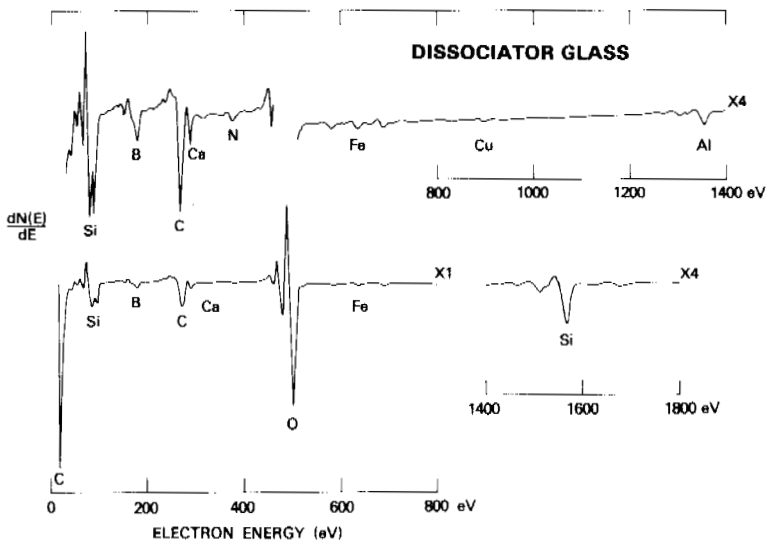

Fig. 4 Typical AES spectrum of dissociator glass.

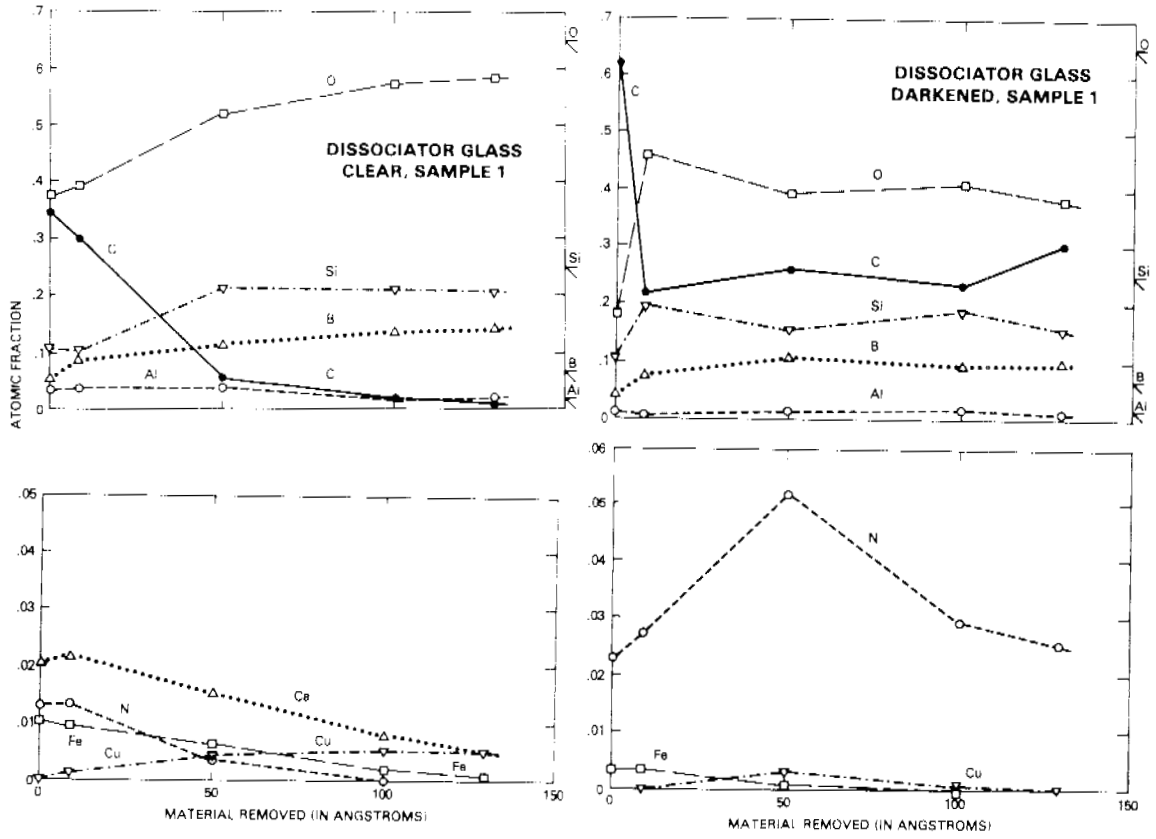

Fig. 5 AES elemental analysis as a function of material removed for the clear and darkened portions of sample 1 (NASA-Goddard).

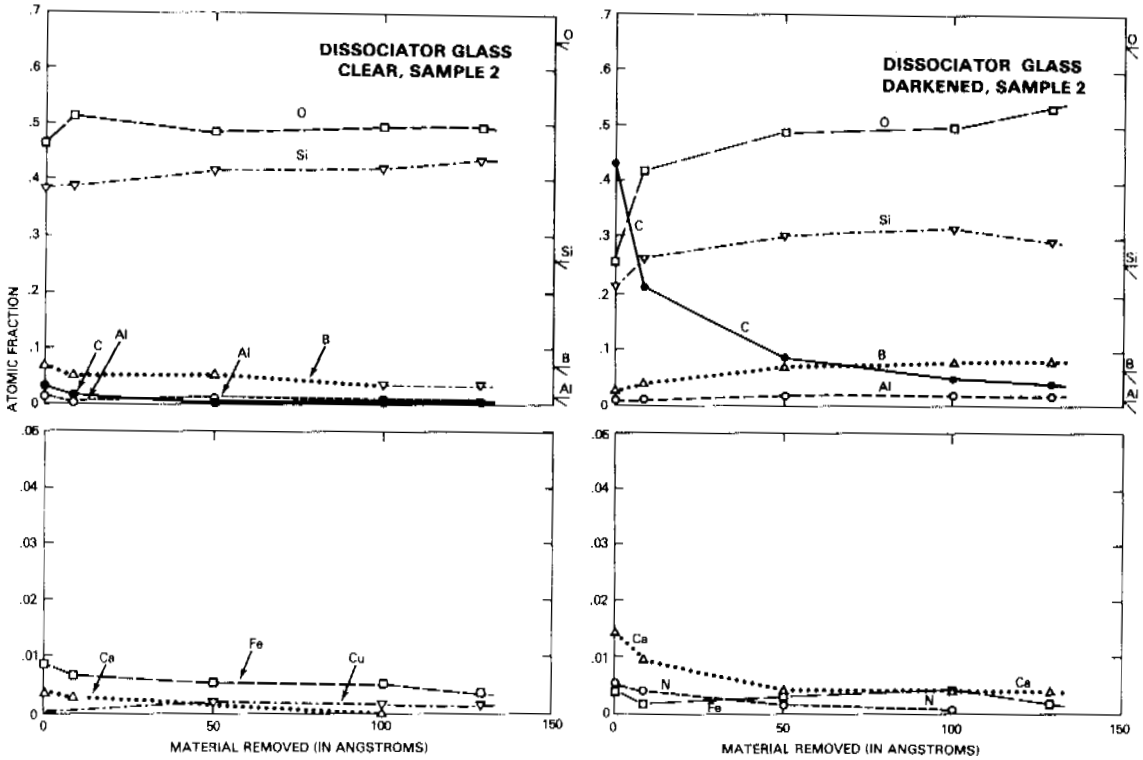

Fig. 6 AES elemental analysis as a function of material removed for the clear (outside) and darkened portions of sample 2 (NASA-Goddard).

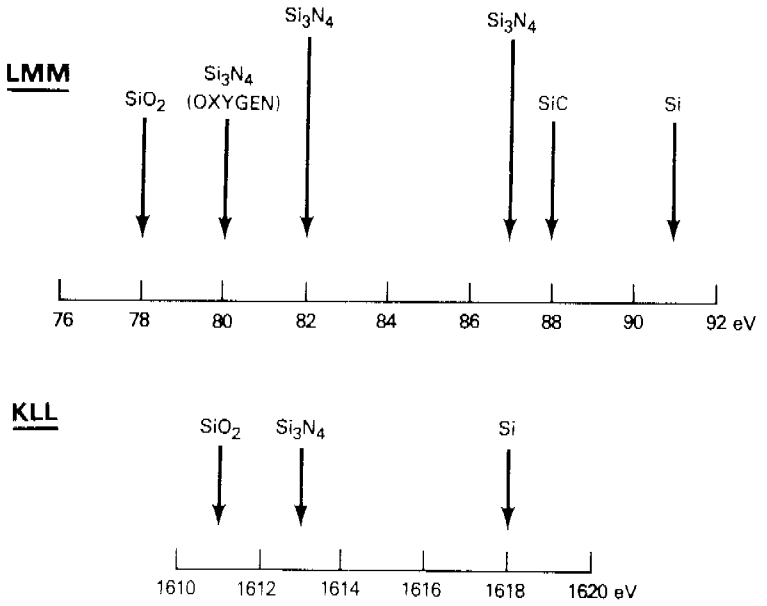

Fig. 7 Chemical bonding shifts for Si.

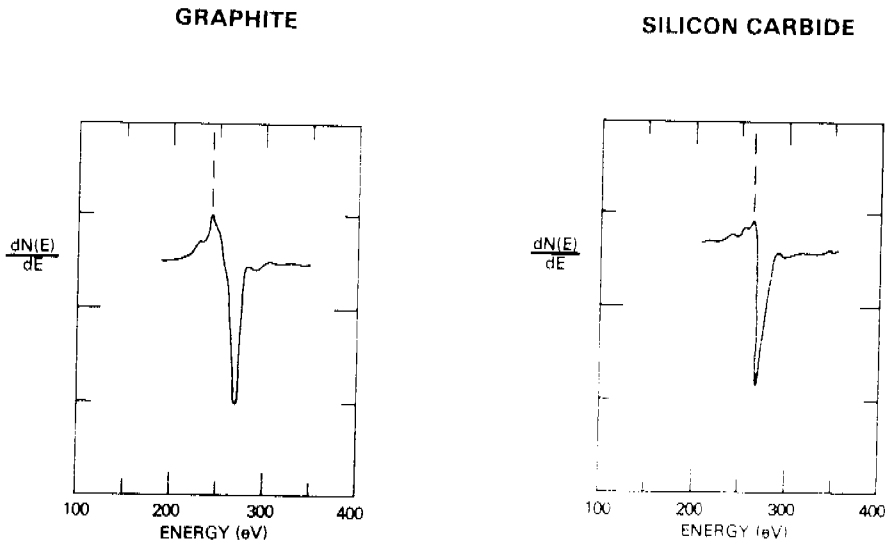

Fig. 8 C Auger peaks in graphite and silicon carbide.

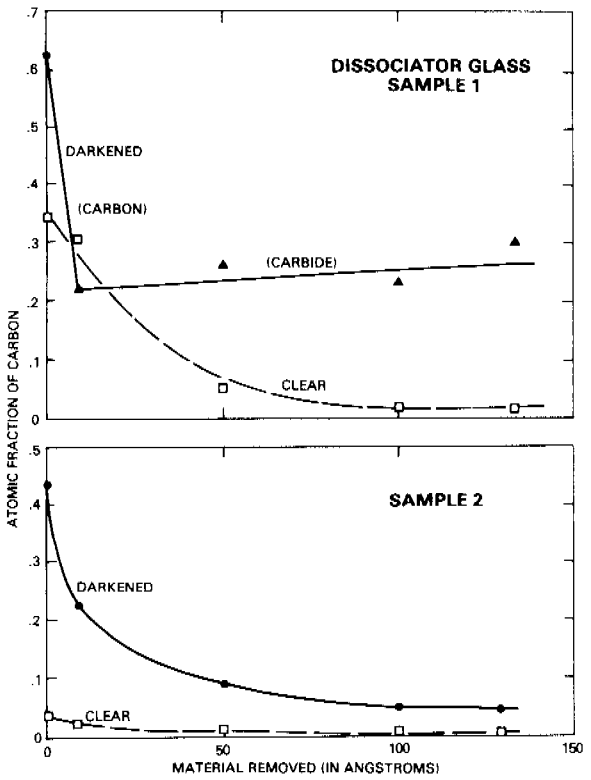

Fig. 9 C content vs depth for NASA-Goddard samples 1 and 2. Solid triangles indicate a "carbide-like" peak. Clear portion of sample 2 analyzed on outside.

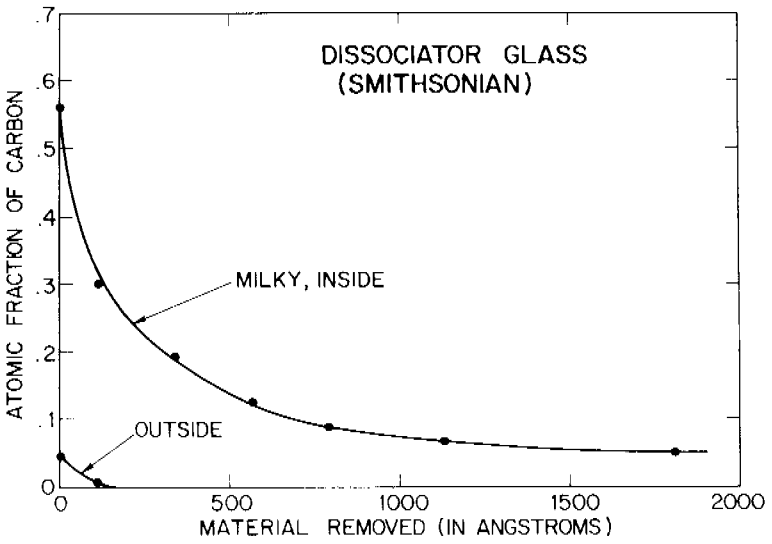

Fig. 10 C content vs depth for a S.A.O. dissociator.

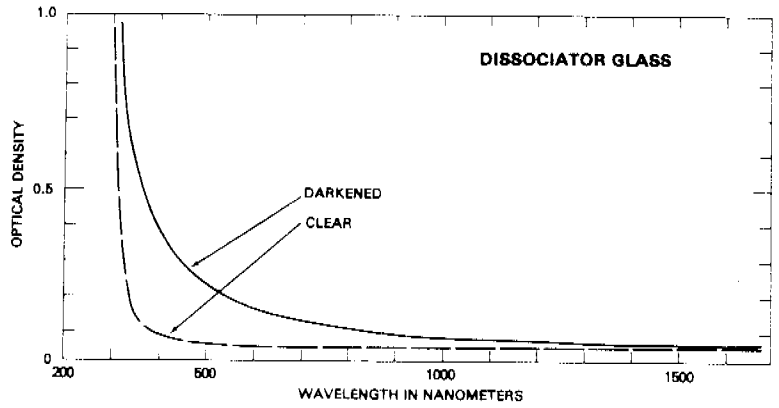

Fig. 11 Optical absorption of the clear and darkened portions of NASA-Goddard dissociator sample 1.

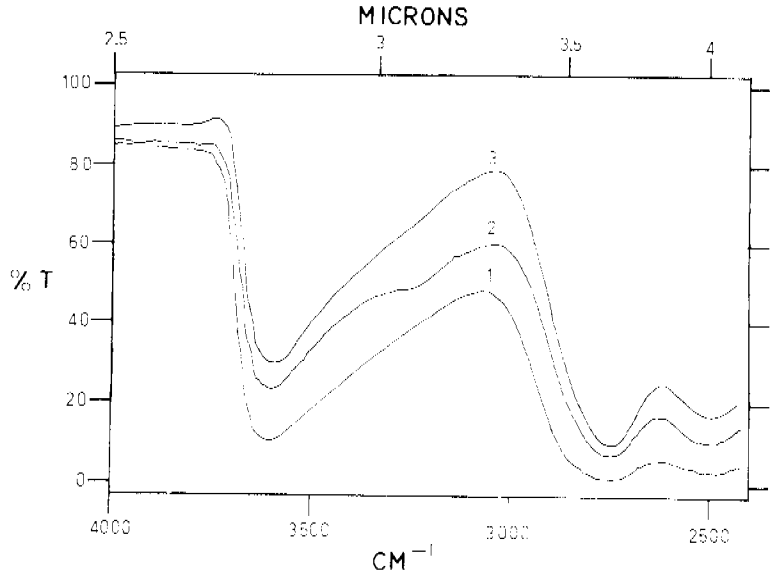

Fig. 12 Percent transmission of clear (1), dark brown (2) and scraped dark brown (3) portions of NASA-Goddard dissociator sample 1.